Transient Expression of Serotonin 5-HT_4 Receptors in the Mouse Developing Thalamocortical Projections

Erin R. Slaten, Melissa C. Hernandez, Ricardo Albay III, Rachel Lavian, Skirmantas Janušonis

Department of Psychology, University of California, Santa Barbara, California 93106-9660

Received 16 August 2009; revised 18 November 2009; accepted 19 November 2009

ABSTRACT: **The serotonin 5-HT_4 receptor (5-HT_4-R) is an unusually complex G-protein coupled receptor that is likely to play important roles in brain development and that may underlie the comorbidity of central and peripheral abnormalities in some developmental disorders. We studied the expression of 5-HT_4-Rs in the developing mouse forebrain at embryonic days 13, 15, 17, and at postnatal days 3 and 14 by using immunohistochemistry, tract tracing, and quantitative RT-PCR. The developing thalamocortical projections transiently expressed 5-HT_4-Rs in the embryonic brain and the 5-HT_4-R expression in the forebrain changed from axonal to somatic around birth. From embryonic days 13–17, the forebrain mRNA levels of the 5-$HT_{4(a)}$-R and 5-$HT_{4(b)}$-R splice variants increased nine- and fivefold, respectively, whereas the levels of the 5-$HT_{4(e)}$-R and 5-$HT_{4(f)}$-R variants remained relatively low throughout the studied period of embryonic development. These results suggest that during development 5-HT_4-R expression undergoes a dynamic regulation and that this regulation may be important for the normal development of sensory and limbic processing.** © 2009 Wiley Periodicals, Inc. Develop Neurobiol 70: 165–181, 2010

Keywords: **5-hydroxytryptamine (5-HT, serotonin); 5-HT_4; thalamocortical; cerebral cortex; development**

INTRODUCTION

The 5-HT_4 receptor (5-HT_4-R) is a G-protein coupled serotonin (5-hydroxytryptamine, 5-HT) receptor that is coded by an unusually large and complex gene (Bockaert et al., 2004, 2006; Barthet et al., 2005). The human 5-HT_4-R gene consists of at least 38 exons, contains the adrenergic β_2 receptor gene within its intron 20, and has a promoter that lacks the TATA- and CAAT-boxes (Bockaert et al., 2004). The 5′-untranslated region (5′-UTR) of the 5-HT_4-R gene contains 25 exons with a part of exon 26 and is likely to be involved in complex translational regulation of 5-HT_4-R expression (Hiroi et al., 2001; Meijer and Thomas, 2002; Maillet et al., 2005). The 5-HT_4-R gene can produce around 10 C-terminal splice variants in humans and pigs (Bockaert et al., 2006; de Maeyer et al., 2008; Ray et al., 2009) and at least four splice variants in mice (Bockaert et al., 2004). The mouse splice variants (5-$HT_{4(a)}$-R, 5-$HT_{4(b)}$-R, 5-$HT_{4(e)}$-R, and 5-$HT_{4(f)}$-R) have high constitutive (agonist-independent) activity and the shorter 5-$HT_{4(e)}$-R and 5-$HT_{4(f)}$-R variants exhibit higher constitutive activity than the 5-$HT_{4(a)}$-R and 5-$HT_{4(b)}$-R variants (Claeysen et al., 1999; Pellissier et al., 2009). In cell culture, mouse 5-HT_4-Rs can activate the extracellular signal-regulated kinase (Erk) pathway independently of G-protein-signaling (Barthet et al., 2007) and, upon agonist stimulation, may be internalized by endocytosis with no recycling (Barthet et al.,

Correspondence to: S. Janušonis (janusonis@psych.ucsb.edu).

Contract grant sponsors: Santa Barbara Cottage Hospital-UCSB Special Research Award, UCSB Academic Senate Research Grants, UCSB URCA Grants.

Published online 8 December 2009 in Wiley InterScience (www.interscience.wiley.com).
DOI 10.1002/dneu.20775

2005). Also, 5-HT_4-Rs can form homodimers or heterodimers with adrenergic β_2 receptors (Berthouze et al., 2005, 2007).

5-HT_4-Rs are expressed in the brain (Bockaert et al., 2006), the pituitary gland (Medhurst et al., 2001), the spinal cord (Millan, 2002), the enteric nervous system (Liu et al., 2005; Mader et al., 2006), the esophagus (Poole et al., 2006), the heart (Bach et al., 2001; Kaumann and Levy, 2006; Lezoualc'h et al., 2007), the bladder (Claeysen et al., 1999), the blood platelets (Amisten et al., 2008; Serebruany et al., 2009), and in some other tissues (Claeysen et al., 1999; Medhurst et al., 2001). In the brain, 5-HT_4-Rs are expressed in neurons, both postsynaptically and presynaptically (Vilaro et al., 2005; Bockaert et al., 2006; Millan et al., 2008), and in astrocytes (Parga et al., 2007; Millan et al., 2008).

In the adult brain, 5-HT_4-Rs have been found in several systems of great functional and clinical importance. In the brainstem, 5-HT_4-Rs play an important role in the pre-Bötzinger complex, a region that generates and controls spontaneous breathing movements (Manzke et al., 2003, 2008). In the rodent forebrain, 5-HT_4-Rs are highly expressed in the dorsal and ventral striatum (the caudate-putamen, the nucleus accumbens, the olfactory tubercle, and the islands of Calleja) and in the hippocampus (Jakeman et al., 1994; Vilaro et al., 1996, 2005; Ullmer et al., 1996; Kornum et al., 2009). In the hippocampus, 5-HT_4-Rs may enhance memory formation (Mohler et al., 2007; Perez-Garcia and Meneses, 2008). They have also been shown to be located on the rat presynaptic terminals of the striato-nigral, dorsal striato-pallidal, ventral striato-pallidal, and habenulo-interpeduncular (fasciculus retroflexus) pathways (Waeber et al., 1993; Vilaro et al., 2005). Activation of 5-HT_4-Rs in the rat prefrontal cortex has a strong excitatory effect on serotonergic neurons in the dorsal raphe nucleus (Lucas et al., 2005), which may be mediated by the direct cortical-raphe projections (Hajos et al., 1998).

The structural and functional complexity of 5-HT_4-Rs suggests that these receptors may be important in brain development. However, their developmental role remains poorly understood. In the embryonic mouse and rat brains, binding studies using [^{3}H]GR113808 as a ligand have found high 5-HT_4-R binding levels in the brainstem but low levels in the forebrain (Waeber et al., 1994, 1996). During the second and third weeks after birth, [^{3}H]GR113808 binding decreases in the brainstem, but it increases and reaches adult-like levels in the forebrain (Waeber et al., 1994). At around 2 weeks after birth, the rat substantia nigra and globus pallidus exhibit transient peaks in [^{3}H]GR113808 binding (Waeber et al., 1994). Interestingly, both of these areas receive afferents that in the adult brain express 5-HT_4-Rs presynaptically (Vilaro et al., 2005), suggesting that 5-HT_4-Rs may be important for the development and maturation of anatomical projections. During late embryonic development (embryonic days 18–20), the 5-HT_4-R immunoreactivity in the rat pre-Bötzinger complex is predominantly present in the neuropil, but after birth the neuropil immunoreactivity rapidly decreases and is replaced by somatic immunoreactivity (Manzke et al., 2008).

Mice lacking functional 5-HT_4-Rs exhibit reduced firing rates in the serotonergic neurons of the dorsal raphe nucleus, lower tissue 5-HT levels in the rostral raphe complex, reduced stress-induced hypophagia, reduced novelty-induced exploratory activity, and increased sensitivity to a seizure-inducing convulsant (Compan et al., 2004; Conductier et al., 2006). These knockout mice also show developmental changes in the enteric nervous system (Liu et al., 2009). Maternal antibodies against 5-HT_4-Rs may lead to various developmental abnormalities in the embryos (Kamel et al., 2007). Activation of astrocytic 5-HT_4-Rs has been shown to inhibit the development of dopaminergic neurons in neurospheres (Parga et al., 2007).

To advance understanding of the role of 5-HT_4-Rs in brain development, we focused on their expression in the developing mouse forebrain. We found that the thalamocortical projections exhibit high but transient 5-HT_4-R expression in the embryonic brain, suggesting that these receptors may be important for the normal development of sensory and limbic processing.

METHODS

Animals

Timed-pregnant CD-1 mice were purchased from Charles River Laboratories (Wilmington, MA) and were housed in individual cages on a 12:12 light–dark cycle (lights on at 07:00, off at 19:00). Mice were inspected in the morning (before 12:00) and the delivery day was considered postnatal day 0. All experiments were approved by the UCSB Institutional Animal Care and Use Committee.

Tissue Harvesting and Histology

At embryonic days (E) 13, 15, and 17, pregnant mice were terminally anesthetized with an overdose of a mixture of ketamine (100 mg/kg) and xylazine (10 mg/kg). Their uterus was dissected and kept in 0.1 *M* phosphate-buffered saline (PBS, pH 7.2) on ice. Embryos were removed from the uterus, immediately decapitated, and their brains were

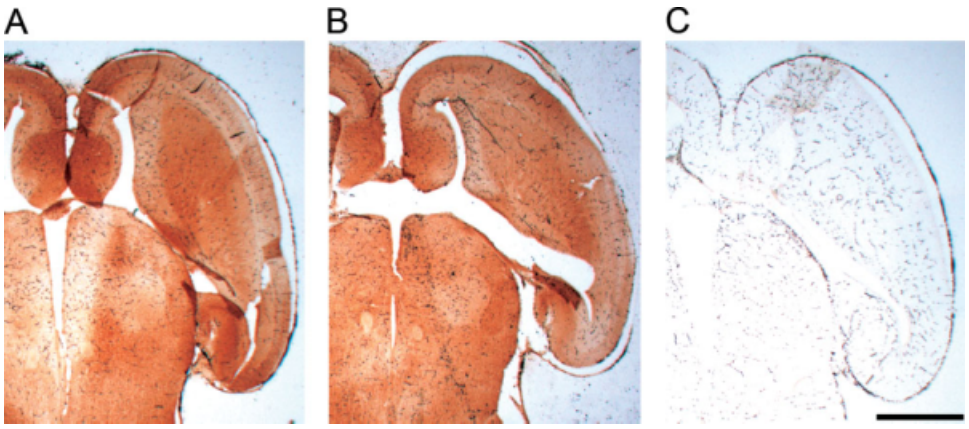

Figure 1 The specificity of the primary anti-5-HT$_4$-R antibody and the secondary biotinylated antibody tested in horizontal E17 sections. All three sections were imaged with the same illumination and camera settings. A: A section stained with the goat anti-5-HT$_4$-R antibody. B: A section stained with the goat anti-5-HT$_4$-R antibody preincubated with the peptide against which it has been raised. Note the signal inhibition in the anterior cortical plate, the striatum, and the hippocampus. C: A section stained with the goat anti-5-HT$_4$-R antibody omitted. Scale bar = 1000 μm. [Color figure can be viewed in the online issue, which is available at www.interscience.wiley.com.]

dissected with fine forceps under a stereoscope. At postnatal days (P) 3 and 14, pups were decapitated and their brains were dissected with fine forceps (P3) or rongeurs (P14).

Brains for immunohistochemistry or Nissl-staining were immersion-fixed overnight in 4% paraformaldehyde or in 4% paraformaldehyde with 2% glutaraldehyde at 4°C, cryoprotected in 30% sucrose at 4°C, and used immediately or stored in a cryoprotectant containing 30% sucrose, 1% polyvinylpyrrolidone (PVP-40), and 30% ethylene glycol in PBS. Brains were embedded in 20% gelatin (bloom 275), incubated for 3 h in formalin with 20% sucrose at room temperature, and sectioned (coronally or horizontally) at 40–50 μm thickness on a freezing microtome. Sections were kept in PBS for immediate processing or stored at −20°C in the cryoprotectant.

Nissl Staining

Sections were rinsed in PBS and water, mounted onto gelatin/chromium-subbed slides, allowed to air-dry, Nissl-stained with 0.25% thionin, dehydrated in a graded series of ethanols, differentiated in 1% glacial acetic acid in 95% ethanol, further dehydrated in absolute ethanol, cleared in xylenes, and coverslipped with Permount.

5-HT$_4$-R and 5-HT Immunohistochemistry

All rinses and incubations were performed at room temperature unless otherwise indicated. For 5-HT$_4$-R immunohistochemistry, sections were rinsed in 0.1 *M* PBS (pH 7.2); blocked for 1 h in 3% normal donkey serum (NDS, Jackson ImmunoResearch) in PBS; incubated for 1–4 days at 4°C in 1:100 (2 μg/mL) goat anti-5-HT$_4$-R IgG (Santa Cruz Biotechnology, sc-32566) with 2% NDS in PBS; rinsed three times (10 min each) in PBS; incubated for 90 min in 1:2000 biotinylated donkey anti-goat IgG (Jackson ImmunoResearch) with 2% NDS in PBS; rinsed three times (10 min each) in PBS; incubated for 1 h in 1:100 avidin-biotin-peroxidase complex (ABC Elite Kit, Vector Labs) in PBS; rinsed three times (10 min each) in PBS; developed for 5 min in 0.05% 3,3′-diaminobenzidine tetrahydrochloride (DAB; ISOPAC, Sigma-Aldrich) with 0.01% H_2O_2 in PBS; rinsed in PBS; mounted onto gelatin/chromium-subbed glass slides and allowed to air-dry; cleared in xylenes and coverslipped with Permount. The specificity of the primary antibody was tested by preincubating the goat anti-5-HT$_4$-R IgG with the peptide against which it has been raised (Santa Cruz Biotechnology, sc-32566P). The antibody and the peptide were incubated overnight at 4°C at the concentrations of 10 and 200 μg/mL, respectively, centrifuged at 21,000*g* for 10 min, and the supernatant was further diluted to the working antibody concentration (2 μg/mL) in PBS with 2% NDS prior to the incubation of sections. The specificity of the secondary antibody was tested at all developmental time points by omitting the primary antibody. The preincubation with the peptide resulted in inhibition of immunoreactivity, which was completely abolished if the primary antibody was omitted (see Fig. 1).

In some sections, immunolabeling was further enhanced (Donovan et al., 2002; Janusonis et al., 2006). Briefly, air-dried sections on slides were incubated for 1 h in 1.42% silver nitrate at 56°C in a water bath; rinsed for 15 min in running deionized water; incubated for 10 min in 0.2% gold chloride in the dark at room temperature; rinsed for 5 min in running deionized water; incubated for 5 min in 5% sodium thiosulfate; rinsed for 10 min in running deionized water; dehydrated in a series of graded ethanols; cleared in xylenes and coverslipped with Permount.

For 5-HT immunohistochemistry, sections were rinsed in PBS, blocked for 30 min in 2% NDS in PBS; incubated

for 1–4 days at 4°C in 1:1000 rabbit anti-5-HT IgG (ImmunoStar, #20080) with 2% NDS, 0.3% Triton X-100 in PBS; rinsed three times (10 min each) in PBS; incubated for 60 min in 1:200 Cy3-conjugated donkey anti-rabbit IgG (Jackson ImmunoResearch) with 2% NDS in PBS; rinsed three times (10 min each) in PBS; mounted onto gelatin/chromium-subbed slides; allowed to air-dry and coverslipped with Cytoseal 60.

5-HT_4-R Immunohistochemistry with Quantum Dots

All rinses and incubations were based on Giepmans et al. (2005) and were performed at 4°C. Sections were rinsed for 15 min in 0.1 *M* PBS (pH 7.2); blocked for 30 min in a blocking buffer containing 3% NDS, 1% cold water fish gelatin (Sigma-Aldrich), and 1% bovine serum albumin (Sigma-Aldrich) in PBS; incubated overnight in 1:100 goat anti-5-HT_4-R IgG (Santa Cruz Biotechnology, sc-32566) in a working buffer (WB, a 1:10 dilution of the blocking buffer); rinsed for 25 min in WB; incubated for 3 h in 1:500 biotinylated donkey anti-goat IgG (Jackson ImmunoResearch) in WB; rinsed for 25 min in WB; incubated in 1:250 quantum dot (QD) 655-conjugated streptavidin (Qdot655, Invitrogen, Q10121MP) in the Qdot incubation buffer (Invitrogen, Q20001MP); and rinsed for 25 min in WB. Sections were stored in WB at 4°C, mounted onto gelatin/chromium-subbed slides, and allowed to air-dry. Sections were examined and imaged uncoverslipped [QD-signal is highly resistant to bleaching (Giepmans et al., 2005)] or coverslipped with Cytoseal 60 (Richard-Allan Scientific). In our hands, Cytoseal 60 was superior to other mounting media (e.g., Permount, Gelvatol) in preserving the QD655-signal. QD655-labeled sections were not counterstained with DAPI because the absorption maxima of both QD655 and DAPI are in the UV-spectrum and DAPI signal rapidly degrades when sections are examined in the QD655 channel.

DiI Tracing

DiI tracing was based on a published methodology (Catalano et al., 1991; Molnar and Cordery, 1999). Two cryoprotected E15 brains were bisected sagittally and small crystals of 1,1′-dioctadecyl-3,3,3′,3′-tetramethylindocarbocyanine perchlorate (DiI) were inserted into the thalamus with a fine insect pin under a stereoscope. After 7 days of incubation in 4% paraformaldehyde at 37°C, the brain halves were embedded and sectioned as described in the "Tissue Harvesting and Histology" section. Sections were mounted onto gelatin/chromium-subbed glass slides, allowed to air-dry, counterstained with DAPI, and imaged.

Microscopy and Imaging

Sections were examined and imaged on a Zeiss Axio Imager Z1 system equipped with standard epifluorescence filter sets, a QD655 (40 nm emission) filter set (Chroma Technology Corporation), and a color Zeiss AxioCam HRc camera. Montages were assembled manually in high digital magnification and the editing of images was limited to global brightness, contrast, and gamma adjustments.

Quantitative RT-PCR

Brains of E13, E15, and E17 embryos were dissected from the skull and their telencephala were isolated by carefully cutting the telencephalon–diencephalon junction with Dumont No. 5 forceps. Total RNA was immediately extracted from the telencephalon with the RNeasy Plus Mini Kit (Qiagen) according to the manufacturer's instructions. To keep the total amount of fresh tissue within the limits recommended by the manufacturer, both telencephalic hemispheres were used from E13 and E15 embryos, but only one hemisphere from E17 embryos. The RNA quality (the A260/A280 ratio) and concentration were measured with a NanoDrop spectrophotometer and the samples were stored at −75°C until further processing.

For each sample, around 100 ng of total RNA was reverse-transcribed to cDNA in a PCR thermocycler using the iScript cDNA Kit (Bio-Rad) according to the manufacturer's instructions. Quantitative PCR analysis of the four 5-HT_4-R splice variants (5-$HT_{4(a)}$-R, 5-$HT_{4(b)}$-R, 5-$HT_{4(e)}$-R, and 5-$HT_{4(f)}$-R) was performed using the MyiQ single color real-time PCR detection system (Bio-Rad). Each PCR reaction (20 μL) was performed in triplicate and contained the cDNA equivalent of $\sim$3 ng RNA, forward and reverse splice variant-specific primers (0.5 μM each; Integrated DNA Technologies), 0.2 m*M* dNTPs, 0.25 U Platinum Taq DNA polymerase (Invitrogen), 0.7× SYBR Green I, and 10 n*M* fluorescein in a PCR buffer containing 10 m*M* Tris-HCl (pH 9.0 at 25°C), 50 m*M* KCl, 2.5 m*M* $MgCl_2$, and 0.1% Triton X-100. The primers were designed in Beacon Designer (Premier Biosoft International, Palo Alto, CA) and are given in Table 1. The amplification conditions were as follows: 94°C (3 min); 45 cycles of 93°C (15 s), 56°C (15 s), 72°C (90 s), 78°C (20 s), and 82°C (20 s); and the product melting curves were obtained by increasing temperature from 60 to 95°C in 0.5°C increments. To minimize nonspecific signal, fluorescence values used in the analysis were obtained at the highest available temperature at which no melting of the product double-stranded DNA was detected. Cycle threshold values (C_t) were obtained from the linear region of baseline-subtracted, log-transformed amplification curves (the same threshold was used for all amplifications). Because of very low levels of some 5-HT_4-R mRNA splice variants (especially at E13), nonspecific products (such as primer-dimers) were detected in some amplifications. The identity of these nonspecific products was confirmed in control amplifications with no template. Amplifications that yielded only nonspecific products or nonspecific products with melting temperatures higher than the analysis temperature were eliminated from the triplicate. Controls with no reverse transcription indicated no contamination with genomic DNA.

Table 1 Quantitative RT-PCR Primers Used in the Study

Target mRNA Accession	Target mRNA	Forward Primer (5′–3′)	Reverse Primer (5′–3′)	Product Length (bp)
Y09587	5-HT$_4$(a)	ATCCTCTGCTGTGATGATGAG	ACTGTGCAAAACTGTATACCTTAG	120
Y09585	5-HT$_4$(b)	CCTGGACAATGACCTAGAAGAC	TTGCCTCTGCTCTTGGAAA	121
Y09588	5-HT$_4$(e)	ATCCTCTGCTGTGATGATGAG	GGAACAGGTCTATTGCGGAAG	134
AJ011369	5-HT$_4$(f)	ACCTGTTCCCGTCTAACTGAG	TAGTAACCTGTTCATGCAGACAC	190
NM_009735 (housekeeping gene)	β_2-Microglobulin (B2M)	GGAGAATGGGAAGCCGAACATAC	AGAAAGACCAGTCCTTGCTGAAG	143
NM_008084 (housekeeping gene)	Glyceraldehyde-3-phosphate dehydrogenase (GAPDH)	AATGTGTCCGTCGTGGATCTGA	AGTGTAGCCCAAGATGCCCTTC	117
NM_019639 (housekeeping gene)	Ubiquitin C (UBC)	GATCTTTGCAGGCAAGCAGCT	TTCTCTATGGTGTCACTGGGCTC	174
NM_013684 (housekeeping gene)	TATA box binding protein (TBP)	GTTGGTGATTGTTGGTTTTAAGGG	GGAAGGCGGAATGTATCTGG	197

We made an effort to make mRNA amounts comparable across different splice variants. The relative mRNA amounts were calculated as $1/(2^{C_t} \times BP \times F)$, where BP is the PCR product length in base pairs and F is a correction factor (0.786–1.000) that accounts for the decrease in SYBR green fluorescence as a function of temperature (Monte Radeke, personal communication). For a given primer pair, BP and F were constant. The obtained 5-HT$_4$ mRNA amounts were normalized to the geometric mean of the mRNA amounts of four housekeeping genes (Table 1). Statistical analysis was performed in SPSS 17.0 (SPSS) and the level of significance was set at $p < 0.05$.

RESULTS

During embryonic development, the mouse telencephalon rapidly increases in size (see Fig. 2). This increase is caused by the proliferation, migration, and maturation of neurons in the telencephalon and by the arrival and maturation of projections from the diencephalon and the brainstem. At E13, a stream of 5-HT$_4$-R-immunoreactive (5-HT$_4$-Rir) fibers was detected in the lateral diencephalon. In horizontal sections, these fibers appeared to abruptly change their direction between the caudal and rostral diencephalon and advance in the caudal–rostral direction in the rostral diencephalon. At the same horizontal level, a stream of 5-HT$_4$-Rir fibers was observed in the striatum; a densely labeled cluster of these fibers appeared to be perpendicular to the

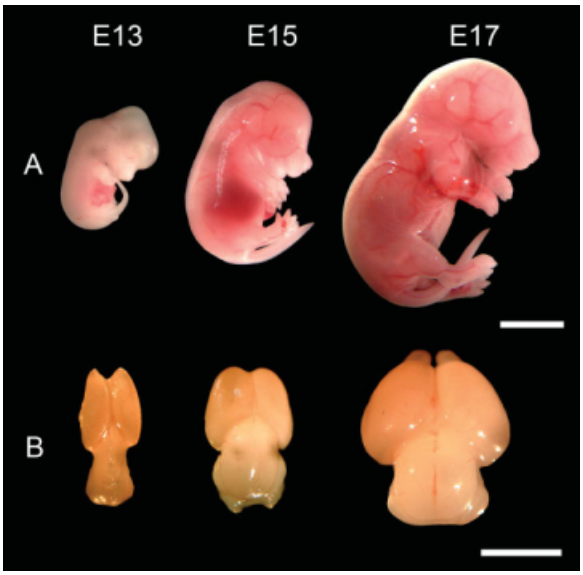

Figure 2 The development of the body (A) and the brain (B) of the CD-1 mouse during embryonic days (E) 13–17. Scale bars = 5 mm in (A) and 3 mm in (B). [Color figure can be viewed in the online issue, which is available at www.interscience.wiley.com.]

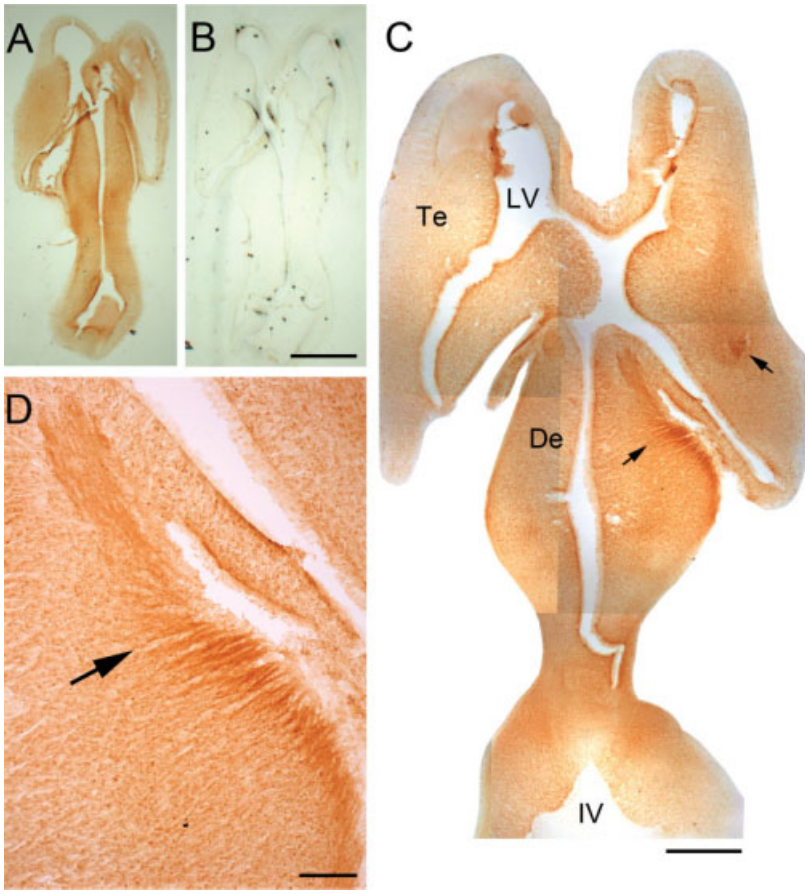

Figure 3 5-HT_4-R immunoreactivity (DAB) in the embryonic mouse brain at E13. (A) A low-magnification image of a horizontal section. (B) A corresponding negative control section. Negative control sections at the later developmental time points also had negligible background immunoreactivity (not shown). (C) A montage of another horizontal section. Note the 5-HT_4-Rir fibers in the lateral diencephalon and in the striatum (arrows). (D) A high-magnification image of the diencephalic 5-HT_4-Rir fibers in (C). These fibers appear to abruptly change their direction between the rostral and caudal diencephalon (arrow). De, diencephalon; IV, fourth ventricle; LV, lateral ventricle; Te, telencephalon. Scale bars = 1000 μm in (A, B); 400 μm in (C); and 100 μm in (D). [Color figure can be viewed in the online issue, which is available at www.interscience.wiley.com.]

horizontal plane (i.e., oriented in the ventral–dorsal direction) (see Fig. 3). This trajectory of the fibers was consistent with the trajectory of the thalamocortical fibers that originate in the dorsal thalamus, pass through the rostrally located ventral thalamus, and make an abrupt turn dorsally before entering the telencephalon (Molnar et al., 1998; Sherman and Guillery, 2006).

Two days later (at E15), strong 5-HT_4-R immunoreactivity was observed in the fibers that originated in the diencephalon and entered the developing striatum (see Fig. 4). In the striatum, these fibers were organized in fascicles that fanned out in a pattern typical of the thalamocortical projections (Molnar et al., 1998) (see Fig. 4). Silver-gold intensification revealed intensely stained 5-HT_4-Rir fibers in the diencephalon-telencephalon junction and in the striatum (see Fig. 5). Upon entering the telencephalon, some 5-HT_4-Rir fibers turned rostrally to reach the frontal cortex and provided dense input to the developing anterior cingulate cortex [Fig. 5(A,D)].

In rodents, the brainstem serotonergic projections arrive in the telencephalon around the same developmental time (Lidov and Molliver, 1982; Wallace and Lauder, 1983; Bruning et al., 1997). Therefore, we next investigated the relationship of these brainstem projections to the 5-HT_4-Rir fibers. At E15, we traced thalamocortical projections with DiI crystals implanted into the thalamus and, in other E15 brains, used 5-HT-immunohistochemistry to reveal the tra-

jectory of the serotonergic fibers in the diencephalon and the telencephalon (see Fig. 6). Most of the 5-HT-immunoreactive (5-HTir) fibers reached the telencephalon by following a straight caudal–rostral trajectory in the ventral forebrain [Fig. 6(F–G)]. In contrast, most of the thalamocortical fibers entering the telencephalon were located more dorsally [Fig. 6(B,C)]. At some horizontal levels, thalamocortical fibers and 5-HTir fibers entered the telencephalon as two adjacent fiber streams [Fig. 6(C,F)]. In the telencephalon, these projections immediately turned rostrally and laterally, respectively, suggesting a possible repulsive interaction between them [Fig. 6(C,F)].

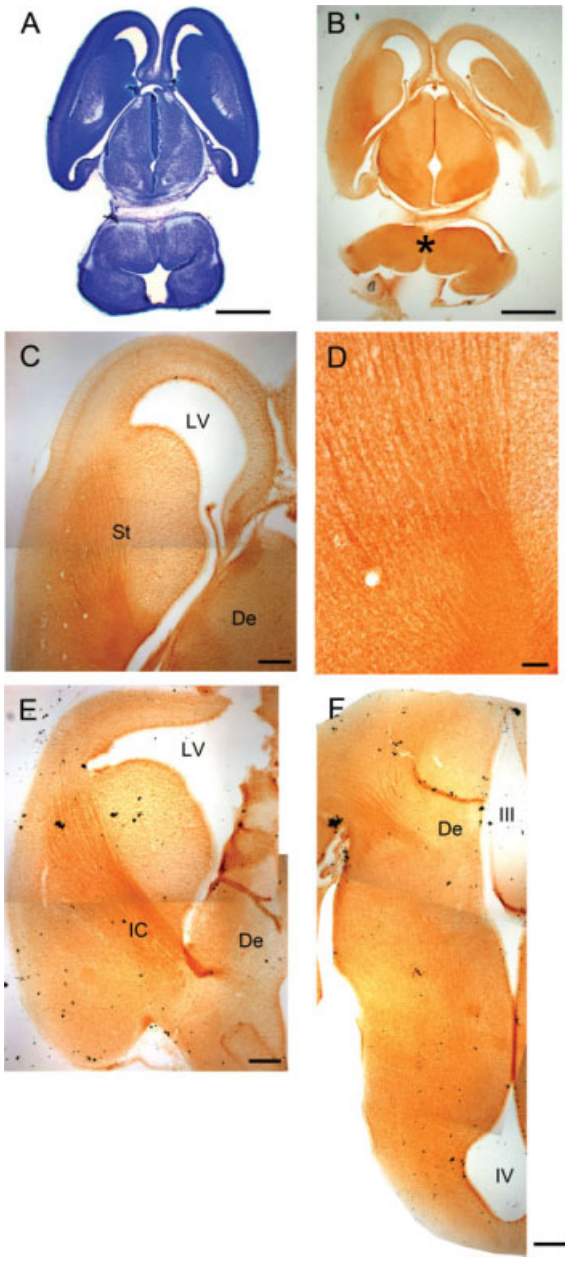

The trajectory of the previously described 5-HT$_4$-Rir fibers was consistent with the trajectory of the thalamocortical fibers and inconsistent with the trajectory of the 5-HTir fibers. The 5-HT$_4$-Rir fibers are unlikely to be corticothalamic because these projections develop later, after E16 in the rat (Molnar and Cordery, 1999).

At E17, the thalamocortical projections exhibited low 5-HT$_4$-immunoreactivity in the diencephalon-telencephalon junction and in the striatum. However, densely stained 5-HT$_4$-Rir fibers were present in the cortical intermediate zone (see Figs. 7 and 8). These fibers were observed in both coronal and horizontal sections at all telencephalic levels. They overlapped with serotonergic (5-HTir) fibers that are also present in the intermediate zone and subplate at this developmental time (Janusonis et al., 2004), but the 5-HTir fibers contained varicosities, were more loosely organized, and did not form well-defined fascicles. Also, another stream of 5-HTir fibers was observed in the cortical marginal zone, as previously described (Janusonis et al., 2004). In contrast, no 5-HT$_4$-Rir fibers were detected in the marginal zone [Fig. 8(F,G)]. Taken together, these results suggest that the 5-HT$_4$R-ir fibers in the intermediate zone were thalamocortical and not serotonergic.

We next tested whether the 5-HT$_4$-Rir fibers could be visualized with QDs. This part of the study was largely methodological, as QDs hold great promise for future correlative light and electron microscopy (Giepmans et al., 2005; Sosinsky et al., 2007), but the reliability of this technique continues to be debated (Resch-Genger et al., 2008). We achieved satisfactory

Figure 4 5-HT$_4$-R immunoreactivity in the embryonic mouse brain at E15. (A) A Nissl-stained horizontal section. (B) A corresponding horizontal section immunostained (DAB) for 5-HT$_4$-R. Note the 5-HT$_4$-Rir fibers in the diencephalon and in the striatum. The strong immunoreactivity in the lower brainstem (asterisk) is consistent with the previous findings of 5-HT$_4$-R binding studies in the embryonic rodent brain (Waeber et al., 1994, 1996). (C) 5-HT$_4$-Rir fibers in the striatum (a high-magnification image of the section in (B)). (D) Fascicles formed by the 5-HT$_4$-Rir fibers in the striatum (a high-magnification of the section in (C)). (E) 5-HT$_4$-Rir (DAB) fibers entering the internal capsule in a horizontal section ventral to the section in (B–D). (F) 5-HT$_4$-R immunoreactivity (DAB) in a horizontal section ventral to the section in (E). Note the virtual absence of somatic immunoreactivity in (B–F). De, diencephalon; IC, internal capsule; III, third ventricle; IV, fourth ventricle; LV, lateral ventricle; St, striatum. Scale bars = 1000 μm in (A, B); 200 μm in (C, E, F); and 50 μm in (D). [Color figure can be viewed in the online issue, which is available at www.interscience.wiley.com.]

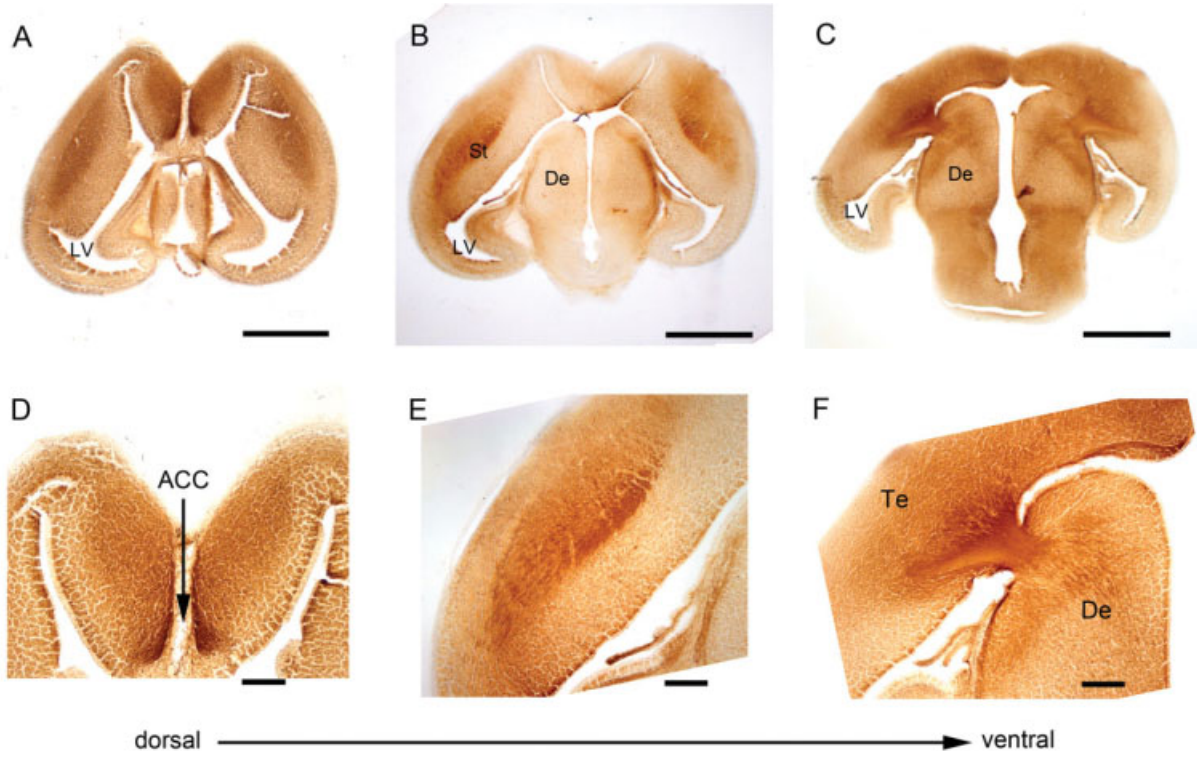

Figure 5 5-HT_4-R immunoreactivity (DAB with silver-gold intensification) in the embryonic mouse brain at E15. (A–C) Low-magnification images of horizontal sections at three different dorsal–ventral levels. (D–F) High-magnification images of the sections in (A–C), respectively. Note high 5-HT_4-R immunoreactivity in the telencephalon–diencephalon junction (C, F), the striatum (B, E), and the anterior cingulate cortex (A, D). ACC; anterior cingulate cortex; De, diencephalon; LV, lateral ventricle; St, striatum; Te, telencephalon. Scale bars = 1000 μm in (A–C) and 200 μm in (D–F). [Color figure can be viewed in the online issue, which is available at www.interscience.wiley.com.]

labeling of 5-HT_4-Rir fibers at E17 with QD655 conjugated to streptavidin [Fig. 8(E)]. This result suggests that 5-HT_4-Rs in the thalamocortical fibers are located in the membrane and are not internalized (Barthet et al., 2005), since QDs are relatively large and cannot readily penetrate the cell membrane (Resch-Genger et al., 2008). It should be noted that QD655-labeled sections had to be imaged within days and, after exposure to mounting media (Permount, Gelvatol, Cytoseal 60), the QD655-signal often deteriorated into a uniform background. Of the three mounting media, Cytoseal 60 gave the best preservation of the signal.

Somatic 5-HT_4-R immunoreactive labeling was virtually absent from the diencephalon and the telencephalon at E13 and was relatively weak at E15. At E17, 5-HT_4-Rir somata were present in the cortical plate; typically, they appeared to be more intensely stained in the lower (developmentally older) cortical layers immediately above the 5-HT_4-Rir fibers [Fig. 8(B,D)]. To study the developmental expression of the four 5-HT_4-R splice variants in the telencephalon, we dissected the telencephala of E13, E15, and E17 mice and analyzed them with quantitative RT-PCR (see Fig. 9 and Table 2). This approach can distinguish the 5-HT_4-R expression in the telencephalic cells from the 5-HT_4-R expression in the axons originating in other brain regions, since distal axons contain no ribosomes and mRNA (Peters et al., 1991; Vilaro et al., 2005). From E13 to E17, we found a ninefold increase in the telencephalic 5-$HT_{4(a)}$ mRNA levels and a fivefold increase in the telencephalic 5-$HT_{4(b)}$ mRNA levels [Fig. 9(D,E)]. No significant change was found in the telencephalic 5-$HT_{4(e)}$ and 5-$HT_{4(f)}$ mRNA levels, which remained very low throughout the studied period of embryonic development [Fig. 9(F,G)].

No 5-HT_4-R immunoreactivity was detected in the thalamocortical fibers postnatally at P3 and P14 (see Fig. 10). At these developmental times, the distribution of 5-HT_4-R immunoreactivity resembled that in the adult rodent brain (Vilaro et al., 2005).

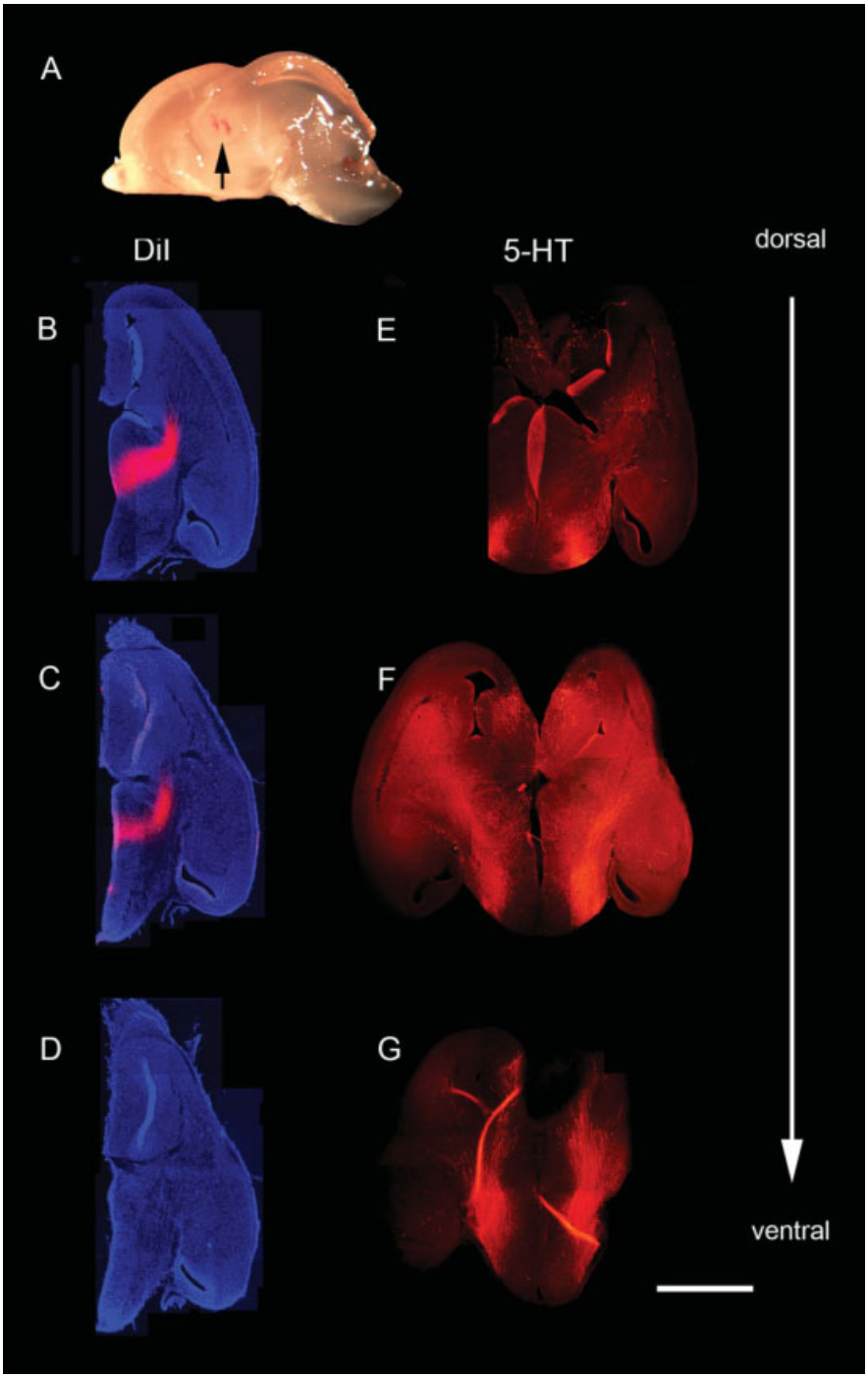

Figure 6 Thalamocortical and serotonergic (5-HTir) projections at E15. (A) DiI crystals implanted in the thalamus (arrow). (B–D) Thalamocortical fibers (DiI, red) in horizontal sections at three different dorsal–ventral levels. The sections have been counterstained with DAPI (blue). (E–G) 5-HTir fibers (Cy3, red) in horizontal sections at three different dorsal–ventral levels corresponding to the levels in (B–D). Note that the majority of the 5-HTir fibers entering the telencephalon are located ventral to the thalamocortical fibers. Scale bar = 1000 μm (in B–G). [Color figure can be viewed in the online issue, which is available at www.interscience.wiley.com.]

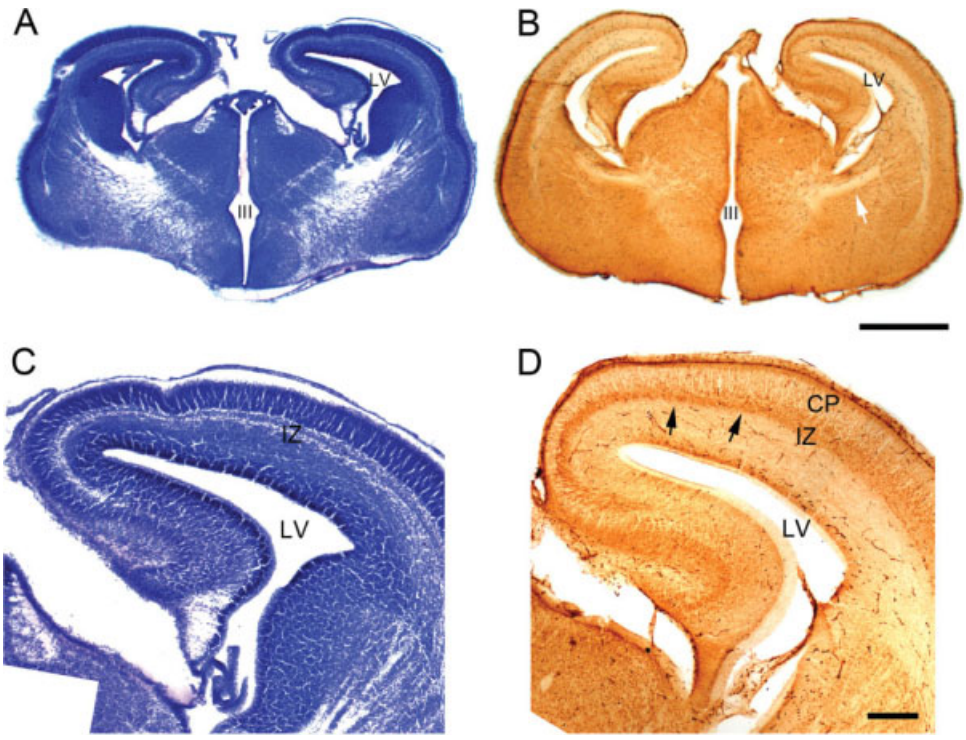

Figure 7 5-HT_4-R immunoreactivity in the embryonic mouse brain at E17. (A) A Nissl-stained coronal section, in which the distribution of the white matter is clearly visible. (B) 5-HT_4-R immunoreactivity (DAB) in a corresponding section. (C, D) High-magnification images of the sections in (A, B). Note the absence of 5-HT_4-R immunoreactivity from the thalamocortical fibers entering the internal capsule (white arrow) and the presence of 5-HT_4-R immunoreactivity in the putative thalamocortical fibers (black arrows) in the cortical intermediate zone (IZ). CP, cortical plate; III, third ventricle; LV, lateral ventricle. Scale bars = 1000 μm in (A, B) and 200 μm in (C, D). [Color figure can be viewed in the online issue, which is available at www.interscience.wiley.com.]

Specifically, high 5-HT_4-R immunoreactivity was found in the piriform cortex, the cortical amygdala, the habenula, the hippocampus, and the hypothalamus. Virtually all 5-HT_4-R immunoreactivity was somatic.

DISCUSSION

A major finding of this study is that the mouse thalamocortical projections transiently express 5-HT_4-Rs during embryonic development. As the 5-HT_4-R-expressing thalamocortical axons spread in the cortical intermediate zone at E17, their proximal segments (located in the thalamus and in the diencephalon-telencephalon junction) begin to lose 5-HT_4-R immunoreactivity and, by postnatal day 3, no 5-HT_4-R immunoreactivity can be detected throughout the thalamocortical axons. This finding suggests that 5-HT_4-Rs may play a role in the growth and/or guidance of the thalamocortical projections. Since the serotonergic projections from the brainstem raphe nuclei reach the telencephalon at approximately the same developmental time as the thalamocortical projections (Lidov and Molliver, 1982; Wallace and Lauder, 1983; Bruning et al., 1997) and the presynaptic elements of the serotonergic projections mature early (Ivgy-May et al., 1994), the 5-HT released from these fibers may be detected by thalamocortical axons that express 5-HT_4-Rs. The exact nature and significance of this interaction remains unclear. Interestingly, the serotonin 5-HT_{1A}, 5-HT_{1B}, 5-HT_{1D}, and 5-HT_{1F} receptors are also transiently expressed in the dorsal thalamus of the embryonic mouse (Bonnin et al., 2006). In embryonic mice 5-HT modulates the response of some thalamocortical fibers to netrin-1; this interaction appears to depend on 5-$HT_{1B/1D}$ receptors (Bonnin et al., 2007).

After having entered the telencephalon, the developing thalamocortical fibers make a sharp dorsal turn (Catalano et al., 1991; Molnar et al., 1998), away from the serotonergic fibers that have already entered the telencephalon but that at this developmental time are located more ventrally (see Fig. 6).

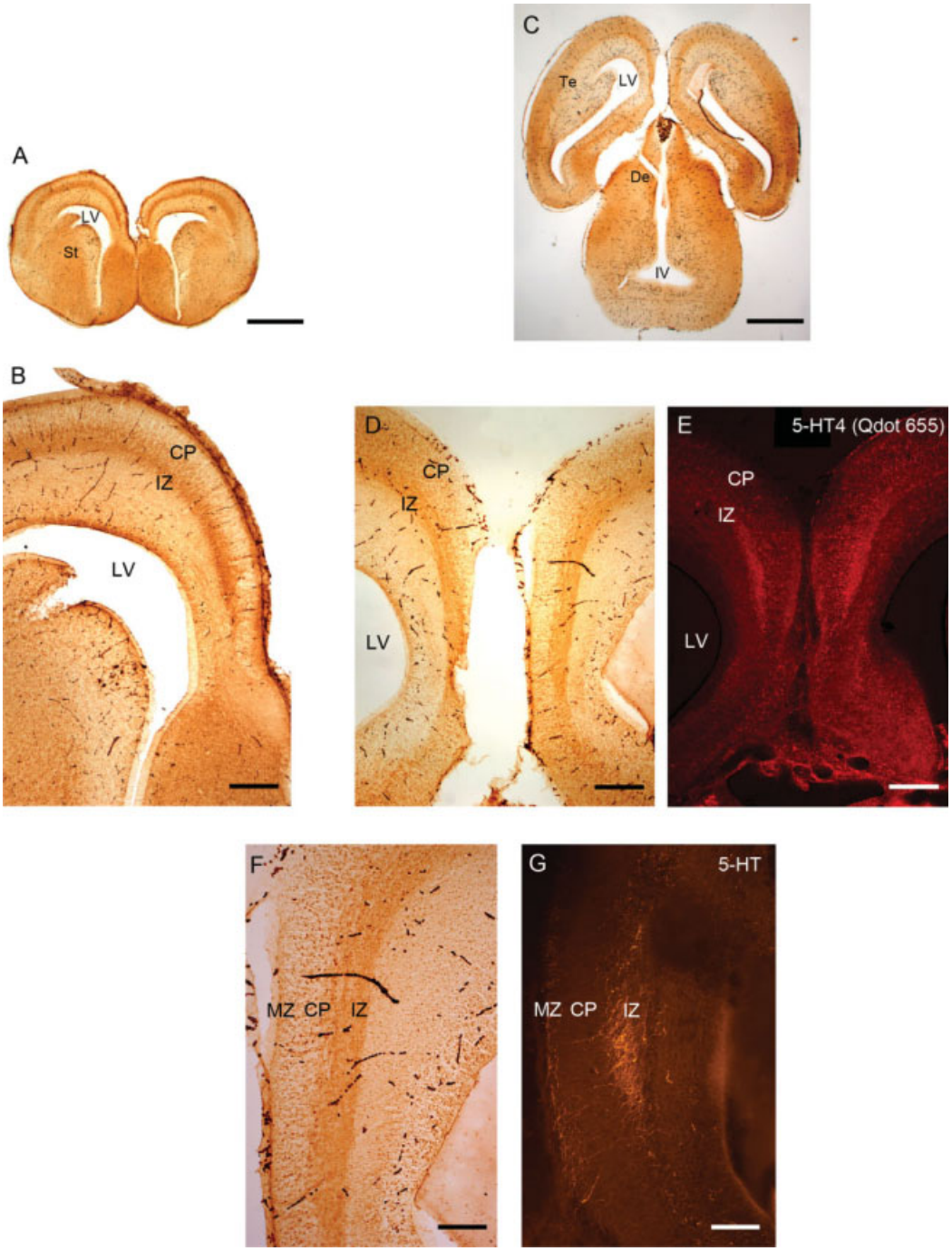

Figure 8 5-HT$_4$-R immunoreactivity in the embryonic mouse brain at E17. (A) 5-HT$_4$-R immunoreactivity (DAB) in a coronal section of the telencephalon. (B) A high-magnification image of the section in (A). (C) 5-HT$_4$-R immunoreactivity (DAB) in a horizontal section. (D) A high-magnification image of the section in (C). (E) 5-HT$_4$-R immunoreactivity (QD655) in a horizontal section. Note that the QD-signal is comparable to the signal produced with DAB as a chromogen. (F) A high-magnification image of the section in (D). (G) Serotonergic (5-HTir) fibers in a comparable horizontal section. In the intermediate zone (IZ), 5-HTir fibers overlap with 5-HT$_4$-Rir fibers, but the overall appearance and distribution of serotonergic fibers is different (also, note the 5-HTir fibers in the marginal zone (MZ) where no 5-HT$_4$-Rir fibers are present). CP, cortical plate; De, diencephalon; IV, fourth ventricle; LV, lateral ventricle; St, striatum; Te, telencephalon. Scale bars = 1000 μm in (A, C); 200 μm in (B, D, E); and 100 μm in (F, G). [Color figure can be viewed in the online issue, which is available at www.interscience.wiley.com.]

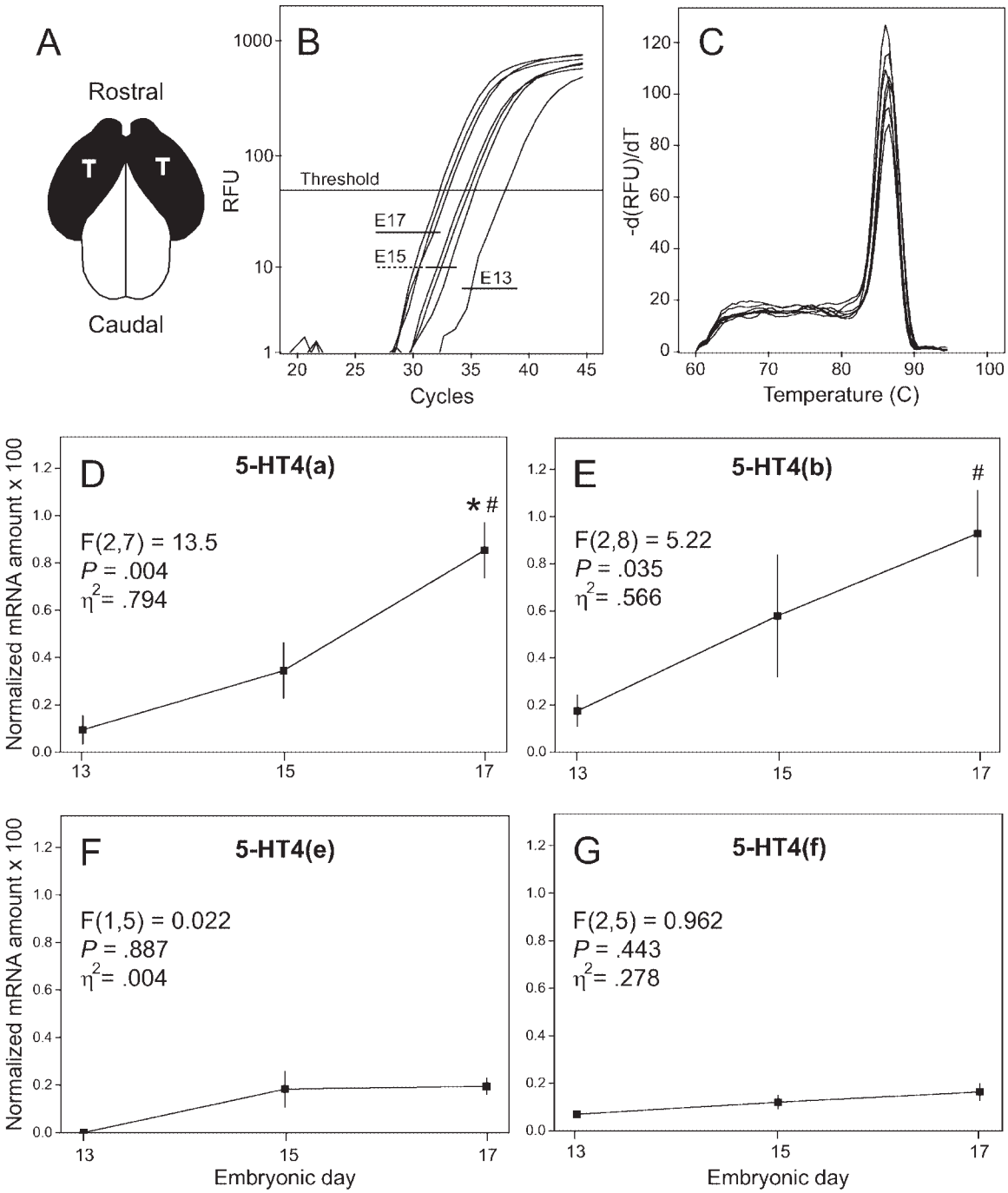

Figure 9 Quantitative RT-PCR analysis of the 5-HT_4-R splice variants in the embryonic telencephalon (E13–E17). (A) The part of the brain used in the analysis (shown in black). (B) Representative, log-transformed amplification curves (5-$HT_{4(a)}$-R) obtained in the same quantitative PCR run. (C) Representative melting curves of the amplification product obtained with the primers specific for the 5-$HT_{4(a)}$-R variant. (D, E) The normalized mRNA amounts of the four mouse 5-HT_4-R splice variants at the three embryonic time points. The error bars are the standard errors of the means. The points marked with # represent a significant *post hoc* difference compared with the point at E13. The point marked with an asterisk (*) represents a significant *post hoc* difference compared with the point at E15. No specific 5-$HT_{4(e)}$-R amplification product was detected at E13; this point was plotted as zero and was not used in the statistical analysis. RFU, relative fluorescence units; –d(RFU)/dT, the negative first derivative of RFU with respect to temperature; T, telencephalon (in A).

Table 2 Statistical Comparison of mRNA Amounts at Three Embryonic Time Points (E13, E15, and E17)

	ANOVA				Regression			
	η^2	F	df	p	R^2	F	df	p
5-HT$_4$(a)	0.794	13.5	2, 7	0.004	0.768	26.5	1, 8	0.0009
5-HT$_4$(b)	0.566	5.22	2, 8	0.035	0.565	11.7	1, 9	0.008
5-HT$_4$(e)	0.004	0.022	1, 5	0.887	0.004	0.022	1, 5	0.887
5-HT$_4$(f)	0.278	0.962	2, 5	0.443	0.277	2.30	1, 6	0.180

Since linear regression is likely to have more statistical power than ANOVA when the independent variable can be measured on a continuous scale (Lazic, 2008), the results of both analyses are given in the table.

Likewise, in horizontal sections, the thalamocortical and serotonergic projections appear to turn away from each other as soon as they leave the narrow diencephalon-telencephalon junction (see Fig. 6). In light of these observations, it is intriguing to speculate that during embryonic development thalamocortical and serotonergic fibers may directly interact. This hypothesis may also shed light on the highly conserved developmental "sandwiching" of the cortical plate between two layers of serotonergic fibers (Lidov and Molliver, 1982; Wallace and Lauder, 1983; Bruning et al., 1997; Verney et al., 2002; Janusonis et al., 2004). By being embedded between two layers of fibers rich in 5-HT, the cortical plate may present a nonpermissive environment to the thalamocortical projections that, at least in some species, can enter the cortical plate only after the "waiting period" in the subplate is over (Rakic, 1977; Kostovic and Rakic, 1990; Ghosh and Shatz, 1992; Molnar et al., 1998).

Since 5-HT$_4$-Rs can exhibit high-constitutive activity (Claeysen et al., 1999; Pellissier et al., 2009) in the absence of a ligand, it is also possible that the expression of 5-HT$_4$-Rs can lead to elevated intracellular cAMP levels even if extracellular 5-HT levels are low. Since the four mouse 5-HT$_4$-R splice variants exhibit different levels of constitutive activity (Claeysen et al., 1999), the exact splice variants expressed by the thalamocortical projections may have important developmental consequences. Addressing this problem directly poses technical challenges, since axons typically do not contain mRNA (Peters et al., 1991; Vilaro et al., 2005) and the cell bodies of thalamocortical neurons are located in the thalamus, in the immediate vicinity of other neurons that do not project to the telencephalon. Obtaining splice-specific *in situ* hybridization signal remains difficult (Vilaro et al., 2005) and, to our knowledge, no specific antibodies currently exist for the 5-HT$_{4(e)}$ and 5-HT$_{4(f)}$ splice variants.

The developing thalamocortical projections are known to transiently express other molecules that detect extracellular 5-HT levels. During early postnatal development in rodents, the thalamocortical neurons transiently express the 5-HT transporter (SERT) that is located on their axons and terminals (Lebrand et al., 1996). It is thought that these neurons use 5-HT as a "borrowed neurotransmitter," since they also express the vesicular monoamine transporter (VMAT2) and their terminals contain 5-HT during early postnatal development (Lebrand et al., 1996). Virtually no SERT is expressed in the embryonic mouse thalamus up until birth (Lebrand et al., 1998), which suggests that the transient SERT expression starts immediately after the transient 5-HT$_4$-R expression ends. It remains unknown if these two processes are functionally related. It should also be noted that the transient SERT expression has not been found in the thalamus of the common marmoset (a primate) (Lebrand et al., 2006), raising a question of whether the transient 5-HT$_4$-R expression is rodent-specific or whether it is present in other mammalian species, including humans.

The potential importance of 5-HT$_4$ receptors in the development of the thalamocortical projections raises questions about the role of these receptors in autism spectrum disorders (ASDs). Individuals with ASDs often show sensory hypersensitivity (Baranek et al., 2007; Gomes et al., 2008), which is intriguing considering that virtually all sensory inputs reach the cerebral cortex by way of thalamocortical projections and that the development of the sensory cerebral cortex is influenced by the thalamic inputs. Also, mice lacking functional 5-HT$_4$-Rs are more prone to seizures than wild-type mice (Compan et al., 2004), which may be due to their abnormal thalamocortical connectivity. Around 25% children with ASDs suffer epileptic seizures (Besag, 2009). Since 5-HT$_4$-Rs play a major role in the development and physiology of the gut (Schworer and Ramadori, 1998; Mader et al., 2006; Liu et al., 2009) and they are also expressed in blood platelets (Amisten et al., 2008; Serebruany et al., 2009), 5-HT$_4$-R abnormalities are also likely to lead to gastrointestinal and blood pathology. The comorbidity of ASDs and gastrointestinal problems has been often reported (Gilger and Redel, 2009), and the

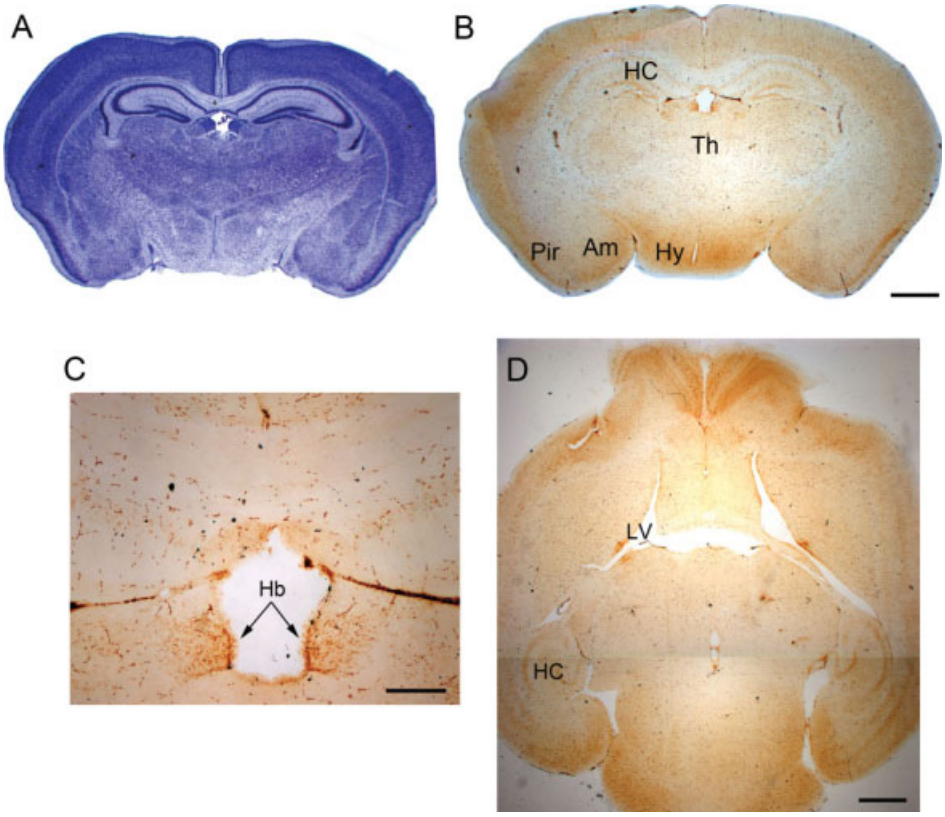

Figure 10 5-HT_4-R immunoreactivity in the postnatal mouse brain at P14. (A) A Nissl-stained coronal section. (B) 5-HT_4-R immunoreactivity (DAB) in a corresponding section. (C) A high-magnification image of the section in (B). (D) 5-HT_4-R immunoreactivity (DAB) in a horizontal section. Am, amygdala; Hb, habenula; HC, hippocampus; Hy, hypothalamus; LV, lateral ventricle; Pir, piriform cortex; Th, thalamus. Scale bars = 1000 μm in (A, B, D); and 200 μm in (C). [Color figure can be viewed in the online issue, which is available at www.interscience.wiley.com.]

elevated 5-HT levels in blood platelets are considered to be one of the most well-replicated biological abnormalities in ASDs (Anderson et al., 1990; Anderson, 2002; Mulder et al., 2004; Janušonis, 2008). Interestingly, both thalamocortical maturation and blood platelet 5-HT levels correlate with body mass in young mice (Hoerder-Suabedissen et al., 2008; Albay et al., 2009).

With respect to the cellular localization of 5-HT_4-R immunoreactivity, the developmental dynamics of the 5-HT_4-R expression in the mouse forebrain is consistent with the findings in the developing rodent brainstem. We found little 5-HT_4-R immunoreactivity in the forebrain somata before E15. Somatic 5-HT_4-R immunoreactivity rapidly increased after E15 and, postnatally, virtually all 5-HT_4-R immunoreactivity was somatic. Another study has reported a similar developmental switch in the rat pre-Bötzinger complex, where most of 5-HT_4-R immunoreactivity is present in the neuropil at E18–E20, but rapidly changes to somatic after birth (Manzke et al., 2008). These results suggest that 5-HT_4-Rs may play a more general role in the development of brain projections. Since the functionality of these receptors is controlled by a large number of post-transcriptional events, current genetic studies in humans may be limited in their ability to detect potential links between altered 5-HT_4-R function and developmental brain disorders.

The authors thank Rebecca Maichrowicz for assistance with brain histology; Angela Chen for assistance developing RT-PCR procedures; and Lincoln Johnson, Monte Radeke, and Natasha Galo for advice on quantitative RT-PCR.

REFERENCES

Albay R, Chen A, Anderson GM, Tatevosyan M, Janusonis S. 2009. Relationships among body mass, brain size, gut length, and blood tryptophan and serotonin in young wild-type mice. BMC Physiol 9:4.

Amisten S, Braun OO, Bengtsson A, Erlinge D. 2008. Gene expression profiling for the identification of G-protein

coupled receptors in human platelets. Thromb Res 122:47–57.

Anderson GM. 2002. Genetics of childhood disorders: XLV. Autism, part 4: Serotonin in autism. J Am Acad Child Adolesc Psychiatry 41:1513–1516.

Anderson GM, Horne WC, Chatterjee D, Cohen DJ. 1990. The hyperserotonemia of autism. Ann NY Acad Sci 600:331–340.

Bach T, Syversveen T, Kvingedal AM, Krobert KA, Brattelid T, Kaumann AJ, Levy FO. 2001. 5HT4(a) and 5-HT4(b) receptors have nearly identical pharmacology and are both expressed in human atrium and ventricle. Naunyn Schmiedebergs Arch Pharmacol 363:146–160.

Baranek GT, Boyd BA, Poe MD, David FJ, Watson LR. 2007. Hyperresponsive sensory patterns in young children with autism, developmental delay, and typical development. Am J Ment Retard 112:233–245.

Barthet G, Carrat G, Cassier E, Barker B, Gaven F, Pillot M, Framery B, et al. 2009. β-arrestin1 phosphorylation by GRK5 regulates G protein-independent 5-HT$_4$ receptor signalling. EMBO J 28:2706–2718.

Barthet G, Framery B, Gaven F, Pellissier L, Reiter E, Claeysen S, Bockaert J, et al. 2007. 5-Hydroxytryptamine 4 receptor activation of the extracellular signal-regulated kinase pathway depends on *Src* activation but not on G protein or β-arrestin signaling. Mol Biol Cell 18:1979–1991.

Barthet G, Gaven F, Framery B, Shinjo K, Nakamura T, Claeysen S, Bockaert J, et al. 2005. Uncoupling and endocytosis of 5-hydroxytryptamine 4 receptors. Distinct molecular events with different GRK2 requirements. J Biol Chem 280:27924–27934.

Berthouze M, Ayoub M, Russo O, Rivail L, Sicsic S, Fischmeister R, Berque-Bestel I, et al. 2005. Constitutive dimerization of human serotonin 5-HT4 receptors in living cells. FEBS Lett 579:2973–2980.

Berthouze M, Rivail L, Lucas A, Ayoub MA, Russo O, Sicsic S, Fischmeister R, et al. 2007. Two transmembrane Cys residues are involved in 5-HT4 receptor dimerization. Biochem Biophys Res Commun 356:642–647.

Besag FM. 2009. The relationship between epilepsy and autism: A continuing debate. Acta Paediatr 98:618–620.

Bockaert J, Claeysen S, Becamel C, Dumuis A, Marin P. 2006. Neuronal 5-HT metabotropic receptors: Fine-tuning of their structure, signaling, and roles in synaptic modulation. Cell Tissue Res 326:553–572.

Bockaert J, Claeysen S, Compan V, Dumuis A. 2004. 5-HT4 receptors. Curr Drug Targets CNS Neurol Disord 3:39–51.

Bonnin A, Peng W, Hewlett W, Levitt P. 2006. Expression mapping of 5-HT$_1$ serotonin receptor subtypes during fetal and early postnatal mouse forebrain development. Neuroscience 141:781–794.

Bonnin A, Torii M, Wang L, Rakic P, Levitt P. 2007. Serotonin modulates the response of embryonic thalamocortical axons to netrin-1. Nat Neurosci 10:588–597.

Bruning G, Liangos O, Baumgarten HG. 1997. Prenatal development of the serotonin transporter in mouse brain. Cell Tissue Res 289:211–221.

Catalano SM, Robertson RT, Killackey HP. 1991. Early ingrowth of thalamocortical afferents to the neocortex of the prenatal rat. Proc Natl Acad Sci USA 88:2999–3003.

Claeysen S, Sebben M, Becamel C, Bockaert J, Dumuis A. 1999. Novel brain-specific 5-HT4 receptor splice variants show marked constitutive activity: Role of the C-terminal intracellular domain. Mol Pharmacol 55:910–920.

Compan V, Zhou M, Grailhe R, Gazzara RA, Martin R, Gingrich J, Dumuis A, et al. 2004. Attenuated response to stress and novelty and hypersensitivity to seizures in 5-HT4 receptor knock-out mice. J Neurosci 24:412–419.

Conductier G, Dusticier N, Lucas G, Cote F, Debonnel G, Daszuta A, Dumuis A, et al. 2006. Adaptive changes in serotonin neurons of the raphe nuclei in 5-HT$_4$ receptor knock-out mouse. Eur J Neurosci 24:1053–1062.

de Maeyer JH, Aerssens J, Verhasselt P, Lefebvre RA. 2008. Alternative splicing and exon duplication generates 10 unique porcine 5-HT$_4$ receptor splice variants including a functional homofusion variant. Physiol Genomics 34:22–33.

Donovan SL, Mamounas LA, Andrews AM, Blue ME, McCasland JS. 2002. GAP-43 is critical for normal development of the serotonergic innervation in forebrain. J Neurosci 22:3543–3552.

Ghosh A, Shatz CJ. 1992. Pathfinding and target selection by developing geniculocortical axons. J Neurosci 12:39–55.

Giepmans BN, Deerinck TJ, Smarr BL, Jones YZ, Ellisman MH. 2005. Correlated light and electron microscopic imaging of multiple endogenous proteins using quantum dots. Nat Methods 2:743–749.

Gilger MA, Redel CA. 2009. Autism and the gut. Pediatrics 124:796–798.

Gomes E, Pedroso FS, Wagner MB. 2008. Auditory hypersensitivity in the autistic spectrum disorder. Pro Fono 20:279–284.

Hajos M, Richards CD, Szekely AD, Sharp T. 1998. An electrophysiological and neuroanatomical study of the medial prefrontal cortical projection to the midbrain raphe nuclei in the rat. Neuroscience 87:95–108.

Hiroi T, Hayashi-Kobayashi N, Nagumo S, Ino M, Okawa Y, Aoba A, Matsui H. 2001. Identification and characterization of the human serotonin-4 receptor gene promoter. Biochem Biophys Res Commun 289:337–344.

Hoerder-Suabedissen A, Paulsen O, Molnar Z. 2008. Thalamocortical maturation in mice is influenced by body weight. J Comp Neurol 511:415–420.

Ivgy-May N, Tamir H, Gershon MD. 1994. Synaptic properties of serotonergic growth cones in developing rat brain. J Neurosci 14:1011–1029.

Jakeman LB, To ZP, Eglen RM, Wong EH, Bonhaus DW. 1994. Quantitative autoradiography of 5-HT4 receptors in brains of three species using two structurally distinct radioligands, [3H]GR113808 and [3H]BIMU-1. Neuropharmacology 33:1027–1038.

Janusonis S. 2008. Origin of the blood hyperserotonemia of autism. Theor Biol Med Model 5:10.

Janusonis S, Anderson GM, Shifrovich I, Rakic P. 2006. Ontogeny of brain and blood serotonin levels in 5-HT1A

receptor knockout mice: Potential relevance to the neurobiology of autism. J Neurochem 99:1019–1031.

Janusonis S, Gluncic V, Rakic P. 2004. Early serotonergic projections to Cajal-Retzius cells: Relevance for cortical development. J Neurosci 24:1652–1659.

Kamel R, Garcia S, Lezoualc'h F, Fischmeister R, Muller S, Hoebek J, Eftekhari P. 2007. Immunomodulation by maternal autoantibodies of the fetal serotoninergic 5-HT4 receptor and its consequences in early BALB/c mouse embryonic development. BMC Dev Biol 7:34.

Kaumann AJ, Levy FO. 2006. 5-Hydroxytryptamine receptors in the human cardiovascular system. Pharmacol Ther 111:674–706.

Kornum BR, Lind NM, Gillings N, Marner L, Andersen F, Knudsen GM. 2009. Evaluation of the novel 5-HT4 receptor PET ligand [11C]SB207145 in the Gottingen minipig. J Cereb Blood Flow Metab 29:186–196.

Kostovic I, Rakic P. 1990. Developmental history of the transient subplate zone in the visual and somatosensory cortex of the macaque monkey and human brain. J Comp Neurol 297:441–470.

Lazic SE. 2008. Why we should use simpler models if the data allow this: Relevance for ANOVA designs in experimental biology. BMC Physiol 8:16.

Lebrand C, Cases O, Adelbrecht C, Doye A, Alvarez C, El MS, Seif I, et al. 1996. Transient uptake and storage of serotonin in developing thalamic neurons. Neuron 17:823–835.

Lebrand C, Cases O, Wehrle R, Blakely RD, Edwards RH, Gaspar P. 1998. Transient developmental expression of monoamine transporters in the rodent forebrain. J Comp Neurol 401:506–524.

Lebrand C, Gaspar P, Nicolas D, Hornung JP. 2006. Transitory uptake of serotonin in the developing sensory pathways of the common marmoset. J Comp Neurol 499:677–689.

Lezoualc'h F, Steplewski K, Sartiani L, Mugelli A, Fischmeister R, Bril A. 2007. Quantitative mRNA analysis of serotonin 5-HT4 receptor isoforms, calcium handling proteins and ion channels in human atrial fibrillation. Biochem Biophys Res Commun 357:218–224.

Lidov HG, Molliver ME. 1982. An immunohistochemical study of serotonin neuron development in the rat: Ascending pathways and terminal fields. Brain Res Bull 8:389–430.

Liu M, Geddis MS, Wen Y, Setlik W, Gershon MD. 2005. Expression and function of 5-HT4 receptors in the mouse enteric nervous system. Am J Physiol Gastrointest Liver Physiol 289:G1148–G1163.

Liu MT, Kuan YH, Wang J, Hen R, Gershon MD. 2009. 5-HT4 receptor-mediated neuroprotection and neurogenesis in the enteric nervous system of adult mice. J Neurosci 29:9683–9699.

Lucas G, Compan V, Charnay Y, Neve RL, Nestler EJ, Bockaert J, Barrot M, et al. 2005. Frontocortical 5-HT(4) receptors exert positive feedback on serotonergic activity: Viral transfections, subacute and chronic treatments with 5-HT_4 agonists. Biol Psychiatry 57:918–925.

Mader R, Kocher T, Haier J, Wieczorek G, Pfannkuche HJ, Ito M. 2006. Investigation of serotonin type 4 receptor expression in human and non-human primate gastrointestinal samples. Eur J Gastroenterol Hepatol 18:945–950.

Maillet M, Gastineau M, Bochet P, Asselin-Labat ML, Morel E, Laverriere JN, Lompre AM, et al. 2005. Functional studies of the 5′-untranslated region of human 5-HT_4 receptor mRNA. Biochem J 387 (Pt 2):463–471.

Manzke T, Guenther U, Ponimaskin EG, Haller M, Dutschmann M, Schwarzacher S, Richter DW. 2003. 5-HT_4(a) receptors avert opioid-induced breathing depression without loss of analgesia. Science 301:226–229.

Manzke T, Preusse S, Hulsmann S, Richter DW. 2008. Developmental changes of serotonin 4(a) receptor expression in the rat pre-Bötzinger complex. J Comp Neurol 506:775–790.

Medhurst AD, Lezoualc'h F, Fischmeister R, Middlemiss DN, Sanger GJ. 2001. Quantitative mRNA analysis of five C-terminal splice variants of the human 5-HT4 receptor in the central nervous system by TaqMan real time RT-PCR. Brain Res Mol Brain Res 90:125–134.

Meijer HA, Thomas AA. 2002. Control of eukaryotic protein synthesis by upstream open reading frames in the 5′-untranslated region of an mRNA. Biochem J 367 (Pt 1):1–11.

Millan MJ. 2002. Descending control of pain. Prog Neurobiol 66:355–474.

Millan MJ, Marin P, Bockaert J, Mannoury la CC. 2008. Signaling at G-protein-coupled serotonin receptors: Recent advances and future research directions. Trends Pharmacol Sci 29:454–464.

Mohler EG, Shacham S, Noiman S, Lezoualc'h F, Robert S, Gastineau M, Rutkowski J, et al. 2007. VRX-03011, a novel 5-HT_4 agonist, enhances memory and hippocampal acetylcholine efflux. Neuropharmacology 53:563–573.

Molnar Z, Adams R, Blakemore C. 1998. Mechanisms underlying the early establishment of thalamocortical connections in the rat. J Neurosci 18:5723–5745.

Molnar Z, Cordery P. 1999. Connections between cells of the internal capsule, thalamus, and cerebral cortex in embryonic rat. J Comp Neurol 413:1–25.

Mulder EJ, Anderson GM, Kema IP, de Bildt A, van Lang ND, den Boer JA, Minderaa RB. 2004. Platelet serotonin levels in pervasive developmental disorders and mental retardation: Diagnostic group differences, within-group distribution, and behavioral correlates. J Am Acad Child Adolesc Psychiatry 43:491–499.

Parga J, Rodriguez-Pallares J, Munoz A, Guerra MJ, Labandeira-Garcia JL. 2007. Serotonin decreases generation of dopaminergic neurons from mesencephalic precursors via serotonin type 7 and type 4 receptors. Dev Neurobiol 67:10–22.

Pellissier LP, Sallander J, Campillo M, Gaven F, Queffeulou E, Pillot M, Dumuis A, et al. 2009. Conformational toggle switches implicated in basal constitutive and agonist-induced activated states of 5-hydroxytryptamine-4 receptors. Mol Pharmacol 75:982–990.

Perez-Garcia G, Meneses A. 2008. Memory formation, amnesia, improved memory and reversed amnesia: 5-HT role. Behav Brain Res 195:17–29.

Peters A, Palay SL, Webster HF. 1991. The Fine Structure of the Nervous System. New York, NY: Oxford University Press, 494 p.

Poole DP, Xu B, Koh SL, Hunne B, Coupar IM, Irving HR, Shinjo K, et al. 2006. Identification of neurons that express 5-hydroxytryptamine4 receptors in intestine. Cell Tissue Res 325:413–422.

Rakic P. 1977. Prenatal development of the visual system in rhesus monkey. Philos Trans R Soc Lond B Biol Sci 278:245–260.

Ray AM, Kelsell RE, Houp JA, Kelly FM, Medhurst AD, Cox HM, Calver AR. 2009. Identification of a novel 5-HT$_4$ receptor splice variant (r5-HT$_{4c1}$) and preliminary characterisation of specific 5-HT$_{4a}$ and 5-HT$_{4b}$ receptor antibodies. Eur J Pharmacol 604:1–11.

Resch-Genger U, Grabolle M, Cavaliere-Jaricot S, Nitschke R, Nann T. 2008. Quantum dots versus organic dyes as fluorescent labels. Nat Methods 5:763–775.

Schworer H, Ramadori G. 1998. Autoreceptors can modulate 5-hydroxytryptamine release from porcine and human small intestine in vitro. Naunyn Schmiedebergs Arch Pharmacol 357:548–552.

Serebruany VL, Mouelhi ME, Pfannkuche HJ, Rose K, Marro M, Angiolillo DJ. Investigations on 5-HT$_4$ receptor expression and effects of tegaserod on human platelet aggregation *in vitro*. Am J Ther, in press.

Sherman SM, Guillery RW. 2006. Exploring the Thalamus and its Role in Cortical Function. Cambridge, MA: The MIT Press, 484 p.

Sosinsky GE, Giepmans BN, Deerinck TJ, Gaietta GM, Ellisman MH. 2007. Markers for correlated light and electron microscopy. Methods Cell Biol 79:575–591.

Ullmer C, Engels P, Abdel'Al S, Lubbert H. 1996. Distribution of 5-HT4 receptor mRNA in the rat brain. Naunyn Schmiedebergs Arch Pharmacol 354:210–212.

Verney C, Lebrand C, Gaspar P. 2002. Changing distribution of monoaminergic markers in the developing human cerebral cortex with special emphasis on the serotonin transporter. Anat Rec 267:87–93.

Vilaro MT, Cortes R, Gerald C, Branchek TA, Palacios JM, Mengod G. 1996. Localization of 5-HT$_4$ receptor mRNA in rat brain by in situ hybridization histochemistry. Brain Res Mol Brain Res 43:356–360.

Vilaro MT, Cortes R, Mengod G. 2005. Serotonin 5-HT$_4$ receptors and their mRNAs in rat and guinea pig brain: Distribution and effects of neurotoxic lesions. J Comp Neurol 484:418–439.

Waeber C, Sebben M, Bockaert J, Dumuis A. 1996. Regional distribution and ontogeny of 5-HT4 binding sites in rat brain. Behav Brain Res 73:259–262.

Waeber C, Sebben M, Grossman C, Javoy-Agid F, Bockaert J, Dumuis A. 1993. [3H]-GR113808 labels 5-HT4 receptors in the human and guinea-pig brain. Neuroreport 4:1239–1242.

Waeber C, Sebben M, Nieoullon A, Bockaert J, Dumuis A. 1994. Regional distribution and ontogeny of 5-HT$_4$ binding sites in rodent brain. Neuropharmacology 33:527–541.

Wallace JA, Lauder JM. 1983. Development of the serotonergic system in the rat embryo: An immunocytochemical study. Brain Res Bull 10:459–479.